Effects of Unbounded External Archive on the Performance of Constrained Multiobjective Evolutionary Algorithms

Yanyu Chen*
Department of Computer Science and Engineering
Southern University of Science and Technology
Shenzhen, China
12210260@mail.sustech.edu.cn

Linfeng Zhu*
Department of Computer Science and Engineering
Southern University of Science and Technology
Shenzhen, China
12211626@mail.sustech.edu.cn

Lie Meng Pang
Department of Computer Science and Engineering
Southern University of Science and Technology
Shenzhen, China
panglm@sustech.edu.cn

Hisao Ishibuchi†
Department of Computer Science and Engineering
Southern University of Science and Technology
Shenzhen, China
hisao@sustech.edu.cn

***Abstract*—External archives have been demonstrated to be an effective technique for evolutionary multiobjective optimization (EMO) algorithms. Conducting subset selection from external archives offers advantages in finding solution sets that outperform the final population. While previous research has examined the impact of external archives on unconstrained multiobjective optimization problems, their effectiveness on constrained multiobjective optimization problems (CMOPs) remains unexplored. This paper investigates the effects of unbounded external archives (UEAs) and three different subset selection methods on the performance of eight constrained EMO algorithms through computational experiments on artificial and real-world CMOPs. Our experimental results demonstrate that UEAs are effective for constrained EMO algorithms in finding solution sets with improved convergence and diversity in comparison with the final population of each algorithm. It is also demonstrated that the effectiveness of UEAs depends on the constraint handling techniques (CHTs) in EMO algorithms and the choice of subset selection method.**

***Index Terms*—Constrained evolutionary multiobjective optimization, Constraint handling techniques (CHTs), Artificial test problems, Real-world problems, Unbounded external archive, Subset selection**

I. Introduction

Constrained multiobjective optimization problems (CMOPs) exist widely in real-world applications. Without loss of generality, a CMOP can be formulated as follows [1]:

$$\begin{aligned} \text{Minimize } \mathbf{f}(\mathbf{x}) &= (f_1(\mathbf{x}), f_2(\mathbf{x}), \ldots, f_m(\mathbf{x}))^T, \\ \text{s.t.} \quad & g_i(\mathbf{x}) \leq 0, \ i = 1, 2, \ldots, k, \\ & h_j(\mathbf{x}) = 0, \ j = 1, 2, \ldots, s, \\ & \mathbf{x} = (x_1, x_2, \ldots, x_n)^T \in \Omega, \end{aligned}$$

where $g_i(\mathbf{x})$ is the ith inequality constraint, $h_j(\mathbf{x})$ is the jth equality constraint, $m,\ k,\ s$ are the number of objectives, inequality constraints and equality constraints, respectively, and $\mathbf{x}$ is a solution vector with n decision variables in the decision space Ω.

The final population is commonly used to evaluate algorithm performance and to serve as a solution set for decision-making. However, it has been demonstrated that the final population often includes dominated solutions [2]. That is, some previously generated and discarded solutions can be better than solutions in the final population. This difficulty can be removed by using an unbounded external archive (UEA) where all the examined solutions are stored [3]. The usefulness of the unbounded external archive was demonstrated in the application of EMO algorithms to real-world problems [4]. The use of the unbounded external archive was also suggested for a fair performance comparison of EMO algorithms under different specifications of population size. Previous research focused on unconstrained EMO algorithms, while the effectiveness of UEAs on constrained EMO algorithms has not been demonstrated yet.

In this paper, we examine the effects of UEAs on eight constrained EMO algorithms with three state-of-the-art constraint handling techniques (CHTs), including the constrained dominance principle (CDP) [5]–[7], the two-stage strategy [8], [9], and the coevolution strategy [10], [11]. Experiments are

*These authors contributed equally to this work.
†Corresponding author.

979-8-3315-3431-8/25/$31.00 ©2025 IEEE

conducted under different specifications of the termination condition and population size using both artificial and real-world CMOPs. Furthermore, we also compare the performance of three different subset selection methods [12]–[14].

The paper is organized as follows. In Section II, eight different constrained EMO algorithms, artificial CMOPs, and real-world CMOPs are explained. Next, the unbounded external archive and three different subset selection strategies are briefly explained in Section III. Then, the experimental settings, results, and analysis are presented in Section IV. Finally, the conclusion is provided in Section V.

II. Preliminaries

A. Compared Constrained EMO Algorithms

Eight constrained EMO algorithms and their CHTs are shown in Table I. Two or three algorithms are selected for each of the three CHTs: CDP, two-stage and coevolution.

TABLE I: Selected Algorithms

Algorithm	Year	CHT
NSGA-II [5]	2002	CDP
C-MOEA/D [6]	2014	CDP
CMME [7]	2023	CDP
PPS [8]	2019	ϵ-constrained and Two-stage
C-TSEA [9]	2021	Two-stage
CMOEA-MS [15]	2022	Two-stage
C-TAEA [10]	2019	Coevolution
CCMO [11]	2021	Coevolution

1) CDP-based algorithms: NSGA-II [5] modifies the Pareto dominance relation using CDP, which always prefers feasible solutions to infeasible solutions. In particular, two solutions $\boldsymbol{x_1}$ and $\boldsymbol{x_2}$ are compared as follows:

- If $\boldsymbol{x_1}$ and $\boldsymbol{x_2}$ are both feasible, they are compared by Pareto dominance.
- If $\boldsymbol{x_1}$ is feasible while $\boldsymbol{x_2}$ is infeasible, $\boldsymbol{x_1}$ is preferred.
- If $\boldsymbol{x_1}$ and $\boldsymbol{x_2}$ are both infeasible, the one with less constraint violation is preferred.

The CHT adopted by C-MOEA/D [6] is similar to CDP. Firstly, all constraints are normalized by dividing each constraint function by the constant term in the constraint. Then, the total constraint violation of each solution $\boldsymbol{x}$ is calculated by adding the normalized violations of inequality and equality constraints. Solutions with smaller total constraint violation are preferred.

CMME [7] utilizes two novel ranking mechanisms. The first ranking mechanism assigns the rank to a solution by CDP, which is combined with a density estimation to enhance mating selection. The second ranking mechanism is used to enhance environmental selection, in which non-dominated sorting is conducted by θ-dominance [16] to strengthen the selection pressure. Additionally, crowding distance and individual density estimation are also used in the enhanced environmental selection to promote diversity.

2) Two-stage-based algorithms: PPS [8] divides the search process into two stages. The population evolves without considering constraints in the first (i.e., push) stage. In the second (i.e., pull) stage, the improved ϵ-constrained is adopted to evolve the population. Different from the original ϵ constraint-handling [17] with a fixed ϵ, in the pull stage of PPS, the ϵ level becomes stricter and increasingly similar to CDP over generations through a self-adaptive mechanism.

C-TSEA [9] also uses a two-stage framework. In the first stage, the population evolves without considering constraints, and an archive is maintained to store feasible solutions. After switching to the second stage, the archive is used as the initial population, and the population evolves with constraints.

CMOEA-MS [15] compares the ratio of feasible solutions in the current population with a threshold λ. Stage A is used when the ratio is smaller than λ, in which the objectives and the constraints are given equal priority. Otherwise, the algorithm changes from stage A to stage B, where the simple CDP gives the objectives lower priority than the constraints.

3) Coevolution-based algorithms: C-TAEA [10] adopts the coevolutionary strategy and maintains two archives: a convergence-oriented archive (CA) and a diversity-oriented archive (DA). CA is updated to optimize both constraints and objectives, while DA is updated without considering any constraints. The two archives cooperate in the process of mating, environmental selection and offspring generation.

Different from other existing coevolutionary frameworks, CCMO [11] is based on a weak cooperation framework, in which the two populations only cooperate in offspring generation. The main population of CCMO is evaluated by the original problem while the subpopulation is evaluated by a simpler helper problem that ignores all constraints of the original problem.

B. Artificial Test Problems

In our computational experiments, we use the following artificial CMOPs test problem suites: MW [18] suite, LIR-CMOP [19] suite and C-DTLZ suite [20]. CMOPs in MW suite are designed with small feasible regions and high convergence difficulties, controlled by a global control process and a local adjustment process. The LIR-CMOP suite employs two types of shape functions to construct both convex and concave Pareto fronts (PFs), and various distance functions [21] to address additional challenges in convergence. The C-DTLZ suite has four three-objective CMOPs. These problems introduce infeasible barriers, rendering a part or all of their Pareto fronts infeasible. All of these artificial test problems have large infeasible regions with complicated geometries, which makes it very difficult for constrained EMO algorithms with simple CHTs to efficiently find their constrained Pareto fronts.

C. Real-world problems

We use CMOPs in the CRE [22] suite and RCM [23] suite as real-world test problems. The CRE suite is an easy-to-use real-world problem suite with eight CMOPs. All problems

in the CRE suite have a small number of decision variables and no equality constraint. The RCM suite contains 50 real-world CMOPs that can be classified into five classes according to their domains. CMOPs in the first three categories of the RCM suite have a small number of decision variables and objectives. CMOPs in the fourth and fifth categories of the RCM suite feature a large number of inequality and equality constraints, respectively, posing difficulties for constrained EMO algorithms in obtaining feasible solutions.

It was reported in [24] that most real-world CMOPs have relatively simple constrained Pareto fronts and do not have large infeasible regions between the constrained and unconstrained Pareto fronts. It was also shown that algorithms perform differently on real-world and artificial CMOPs due to distinct problem features. In this paper, we show the effectiveness of archiving and subset selection using both artificial and real-world CMOPs.

III. Archiving and Subset Selection Strategies

The unbounded external archive (UEA) is used for this paper, which stores all non-dominated feasible solutions generated during the execution of the algorithm. Whereas the maintenance of a large archive in every generation (i.e., the dominance check of all solutions in every generation) is time-consuming, the choice of non-dominated solutions from all the examined solutions after the execution of an EMO algorithm can be quickly completed as explained in [3]. The performance of the final population is compared with a solution set selected from the unbounded external archive (SUEA) [25]. Since the performance of SUEA depends on the choice of subset selection method, we also examine the performance of the following three different subset selection strategies.

A. Greedy distance-based subset selection

Greedy distance-based subset selection (DSS) aims to select solutions one by one to maximize the minimum Euclidean distance between the selected solutions. Among all solutions that are not in the selected subset, the solution to be selected should have the largest distance value to the solutions in the selected subset. Let us denote all non-dominated solutions (i.e., candidate solutions) in the UEA as S_{All}, and the selected subset as S. The first solution is selected from S_{All}, which is usually an extreme solution (i.e., the largest or the smallest) of one of the m-objectives. The second solution is the solution with the largest distance from the first solution. The third solution is the solution with the largest distance to the selected solution set. In this manner, the required number of solutions are selected one by one in a greedy manner. The distance from each unselected solution x (i.e., each solution x in $S_{All} \setminus S$) to the selected solution set S is defined by the minimum distance from x to each selected solution as follows:

$$\begin{aligned} Distance(x, S) &= \min \{\|f(x) - f(x_i)\|, x_i \in S\} \\ &for\ x \in (S_{\text{All}} \setminus S) \end{aligned} \quad (1)$$

B. Greedy HV subset selection

Greedy HV subset selection (LGI-HSS) aims to select a subset of solutions that maximizes the hypervolume indicator [26]. The algorithm iteratively chooses the solution with the largest hypervolume contribution (HVC) one by one until the desired subset size is reached. The HVC value of a solution p to a solution set S is calculated as:

$$HVC(p, S) = HV(S \cup \{p\}) - HV(S), \quad (2)$$

where HV($\cdot$) is the hypervolume value of a solution set.

C. Greedy IGD+ subset selection

Greedy IGD+ subset selection (LGI-IGDSS) aims to select a subset of solutions that minimizes the IGD+ indicator [27]. The original algorithm is used for the IGD indicator but can be changed for the IGD+ indicator by using IGD+ distance instead of Euclidean distance. The core idea of LGI-IGDSS is the same as that of LGI-HSS. The algorithm chooses the solution with the largest IGD+ improvement (IGDpI) one by one until the required number of solutions are selected. The IGDpI value of a solution p to a solution set S is calculated as:

$$IGDpI(p) = IGDp(S, R) - IGDp(S \cup \{p\}, R), \quad (3)$$

where $IGDp(S, R)$ is the IGD+ value of the solution set S with respect to the reference point set R defined as:

$$IGDp(S, R) = \frac{1}{|R|} \sum_{r \in R} \min_{s \in S} \sqrt{\sum_{i=1}^{m} (\max\{0, s_i - r_i\})^2}, \quad (4)$$

where $s = (s_1, s_2, \ldots, s_m)$ is the objective vector of solution s in the solution set S, and $r = (r_1, r_2, \ldots, r_m)$ is the objective vector of reference point r in the reference point set R.

IV. Performance Analysis

A. Experimental Settings

In our computational experiments, both artificial and real-world CMOPs are used to evaluate the effectiveness of UEAs for the eight constrained EMO algorithms. Given that many real-world problems have a relatively small number of decision

TABLE II: Real-World Problems and Settings

Problem	m	n	k	s
CRE2-3-1	2	3	3	0
CRE2-7-4	2	7	11	0
CRE2-4-5	2	5	1	0
CRE3-7-1	3	7	10	0
CRE3-6-2	3	6	9	0
RCM11	5	3	7	0
RCM12	2	4	1	0
RCM13	3	7	11	0
RCM25	2	2	2	0
RCM30	2	25	24	0
RCM50	2	6	0	1

TABLE III: HVIR for the eight selected algorithms on the artificial problems.

Problem	Termination	CCMO	CTAEA	NSGAII	CMOEAD	PPS	CTSEA	CMME	CMOEA-MS
MW8	500	0.000	0.000	0.000	0.017	NaN	0.000	0.011	0.006
	5000	0.031	0.088	0.046	0.042	0.079	0.029	0.083	0.024
	50 000	0.015	0.046	0.070	0.018	0.122	0.014	0.046	0.015
	100 000	0.015	0.048	0.072	0.018	0.108	0.015	0.047	0.015
MW10	500	0.000	0.000	−0.003	0.120	0.017	−0.002	0.003	0.044
	5000	0.000	0.006	0.001	0.010	0.004	0.000	0.007	0.001
	50 000	0.001	0.003	0.002	0.003	0.003	0.001	0.004	0.001
	100 000	0.001	0.004	0.002	0.002	0.002	0.001	0.004	0.001
MW12	500	0.000	0.003	0.000	0.011	0.000	0.000	0.000	0.039
	5000	0.002	0.008	0.003	0.012	0.005	0.002	0.005	0.398
	50 000	0.001	0.007	0.004	0.000	0.005	0.001	0.002	0.002
	100 000	0.001	0.007	0.004	0.000	0.005	0.001	0.001	0.002
MW14	500	0.005	0.009	0.001	0.111	0.034	0.001	0.012	0.263
	5000	0.021	0.025	0.030	0.104	0.039	0.018	0.053	0.033
	50 000	0.024	0.038	0.067	0.101	0.056	0.023	0.043	0.039
	100 000	0.026	0.040	0.073	0.098	0.058	0.026	0.044	0.039
LIR-CMOP1	500	0.000	NaN	0.000	0.000	∞	0.000	0.000	0.000
	5000	0.000	0.000	0.000	0.087	0.076	0.000	0.000	0.000
	50 000	0.005	0.000	0.000	0.144	0.005	0.000	0.000	0.000
	100 000	0.000	0.000	0.000	0.127	0.007	0.000	0.003	1.295
LIR-CMOP5	500	0.000	0.000	0.000	0.005	0.011	0.000	0.000	0.000
	5000	0.001	0.003	0.000	0.002	0.010	0.001	0.003	0.001
	50 000	0.002	0.008	0.003	0.006	0.006	0.003	0.010	0.002
	100 000	0.003	0.013	0.004	0.007	0.006	0.003	0.011	0.002
LIR-CMOP7	500	0.000	0.003	0.000	0.046	0.616	0.001	0.015	0.087
	5000	0.004	0.005	0.007	0.099	0.021	0.004	0.013	0.123
	50 000	0.003	0.008	0.007	0.007	0.007	0.003	0.009	0.003
	100 000	0.003	0.012	0.008	0.007	0.008	0.003	0.007	0.004
LIR-CMOP9	500	0.000	0.077	0.006	3.415	5.255	0.011	0.040	0.011
	5000	0.000	0.012	0.000	0.289	0.003	0.000	0.004	0.010
	50 000	0.000	0.011	0.000	0.026	0.001	0.000	0.002	0.089
	100 000	0.000	0.013	0.000	0.015	0.000	0.000	0.002	0.044
LIR-CMOP10	500	0.000	0.031	0.239	0.934	0.768	0.000	1.424	0.062
	5000	0.001	0.006	0.001	0.395	0.004	0.001	0.004	0.002
	50 000	0.000	0.007	0.001	0.017	0.001	0.001	0.004	0.009
	100 000	0.001	0.008	0.001	0.031	0.001	0.001	0.003	0.014
LIR-CMOP14	500	0.000	0.000	0.000	0.003	0.010	0.000	0.000	0.000
	5000	0.435	0.000	1.059	3.429	2.024	−0.055	0.000	0.297
	50 000	0.028	0.042	1.291	0.083	0.099	0.026	0.418	0.034
	100 000	0.027	0.043	3.186	−0.017	0.075	0.026	3.950	0.025
C1-DTLZ1	500	NaN	NaN	NaN	0.408	NaN	NaN	NaN	NaN
	5000	0.006	0.009	0.003	0.033	NaN	0.007	0.000	0.000
	50 000	0.024	0.002	0.002	0.026	0.001	0.004	0.002	0.007
	100 000	0.001	0.007	0.024	0.002	0.025	0.001	0.002	0.004
C3-DTLZ4	500	0.041	0.215	0.031	0.777	0.006	0.032	0.019	0.020
	5000	0.043	0.023	0.021	0.058	0.010	0.283	0.016	0.018
	50 000	0.044	0.005	0.015	0.036	0.011	0.500	0.011	0.015
	100 000	0.014	0.016	0.046	0.005	0.036	0.011	0.016	0.584

variables (n) and two objectives (m = 2), the number of decision variables (n) is specified as $n = 6$ in all two-objective test problems in the MW [18] and LIR-CMOP [19] suites. For three-dimensional artificial test problems, n is specified as 15 for MW8, and MW14, $n = 30$ for LIR-CMOP14, $n = 7$ for C1-DTLZ1 and $n = 12$ for C3-DTLZ4.

As real-world CMOPs, problems in Table II are selected from the CRE [22] and RCM [23] suites. In Table II, k is the number of inequality constraints, and s is the number of equality constraints. Some real-world problems have a large number of constraints. Those problems are excluded from our computational experiments since almost all constrained EMO algorithms cannot find feasible solutions (i.e., no feasible solutions are stored in UEAs).

All experiments are conducted in PlatEMO [28] and the parameter settings for each algorithm are set as default in PlatEMO. 21 independent runs are conducted for each algorithm. The HV values of the final population (FPOP) and the selected subset (SUEA) from the UEA will be compared in the subsequent analysis.

1) Settings for constrained EMO algorithms: The maximum number of solution evaluations and the population size (N) are set as follows:

- Number of solution evaluations = 500, N = 20;
- Number of solution evaluations = 5000, N = 50;
- Number of solution evaluations = 50000, N = 100;
- Number of solution evaluations = 100000, N = 100;

LGI-HSS [13] is used for experiments under the three conditions, and the reference point is specified as $(1 + 1/H) \times (1, \ldots, 1)$, where H is set to 99, 12, and 4 for $m = 2,\ 3,\ and\ 5$, respectively, as suggested in [29].

2) Settings for subset selection strategies: The three subset selection algorithms (DSS, LGI-HSS, and LGI-IGDSS) are used to select 100 solutions from non-dominated solutions in the UEA after each run of each constrained EMO algorithm on each problem. Before subset selection, all dominated solutions are removed from the UEA.

B. Experimental Results

The hypervolume improvement rate (HVIR) is used to measure the effectiveness of SUEA. The average HVIR over 21 runs of each algorithm on each problem is calculated as:

$$HVIR(SUEA) = \underset{j=1,\ldots,21}{ave}\left(\frac{HV_j(SUEA) - HV_j(FPOP)}{HV_j(FPOP)} \times 100\right). \tag{5}$$

In some cases (especially when the number of examined solutions is small), the HV value is zero since the obtained solutions are not close to the Pareto front. For those cases, the reference point for calculating HV value is multiplied by 100

TABLE IV: HVIR for the eight selected algorithms on the real-world problems.

Problem	Termination	CCMO	CTAEA	NSGAII	CMOEAD	PPS	CTSEA	CMME	CMOEA-MS
CRE2-3-1	500	0.000	0.000	0.000	0.024	∞	0.000	0.001	0.027
	5000	0.007	0.000	0.003	19.485	0.020	0.007	0.010	0.084
	50 000	0.004	0.000	0.001	65.501	0.039	0.005	0.005	0.052
	100 000	0.004	0.001	0.001	59.545	0.034	0.005	0.005	0.048
CRE2-7-4	500	0.062	0.000	0.000	0.052	0.122	0.000	0.000	0.050
	5000	0.000	0.000	0.000	0.002	0.001	0.000	0.001	0.054
	50 000	0.001	0.001	0.001	0.001	0.001	0.001	0.001	0.128
	100 000	0.002	0.001	0.001	0.001	0.001	0.002	0.001	0.002
CRE2-4-5	500	0.000	0.002	0.000	0.157	0.247	0.000	0.004	0.000
	5000	0.000	0.001	0.000	0.012	0.002	0.000	0.001	0.000
	50 000	0.000	0.001	0.000	0.008	0.000	0.000	0.001	0.000
	100 000	0.000	0.002	0.000	0.007	0.000	0.000	0.002	0.000
CRE3-7-1	500	0.071	0.131	0.097	6.107	0.087	0.073	0.089	0.078
	5000	0.063	0.056	0.099	7.155	0.124	0.071	0.067	0.064
	50 000	0.051	0.052	0.087	4.922	0.116	0.053	0.052	0.049
	100 000	0.053	0.055	0.084	5.707	0.125	0.054	0.052	0.049
CRE3-6-2	500	0.000	0.004	0.000	0.240	0.176	0.000	0.015	0.097
	5000	0.002	0.015	0.005	0.140	0.263	0.002	0.029	0.566
	50 000	0.004	0.021	0.012	0.138	0.015	0.005	0.023	0.495
	100 000	0.006	0.020	0.012	0.135	0.016	0.005	0.023	0.540
RCM11	500	0.202	0.133	0.248	0.270	0.289	0.172	0.155	0.154
	5000	0.094	0.096	0.104	0.364	0.080	0.095	0.202	0.082
	50 000	0.063	0.061	0.061	0.548	0.039	0.065	0.106	0.134
	100 000	0.066	0.063	0.063	0.568	0.038	0.064	0.099	0.129
RCM12	500	0.003	0.014	−0.002	1.596	0.028	0.002	0.004	0.160
	5000	0.005	0.018	0.003	10.545	0.014	0.005	0.007	0.176
	50 000	0.004	0.009	0.002	1.364×10^3	0.008	0.005	0.005	0.360
	100 000	0.006	0.011	0.002	63.058	0.008	0.007	0.005	0.343
RCM13	500	0.001	0.005	0.010	0.520	0.368	0.002	0.011	0.087
	5000	0.022	0.005	0.019	0.034	0.019	0.021	0.005	0.156
	50 000	0.025	0.012	0.013	0.011	0.020	0.027	0.013	0.118
	100 000	0.026	0.013	0.013	0.012	0.029	0.027	0.014	0.214
RCM25	500	0.004	0.011	0.029	0.414	0.141	0.003	0.005	0.020
	5000	−0.001	0.002	0.007	0.060	0.006	−0.001	0.002	0.034
	50 000	−0.001	0.001	0.003	0.028	0.002	−0.001	0.001	0.036
	100 000	−0.001	0.000	0.003	0.028	0.002	−0.001	0.001	0.036
RCM30	500	NaN	NaN	NaN	NaN	NaN	NaN	NaN	NaN
	5000	NaN	NaN	NaN	NaN	NaN	NaN	NaN	NaN
	50 000	0.000	0.000	0.001	0.110	0.002	0.000	0.000	NaN
	100 000	0.000	0.004	0.000	0.019	0.003	0.000	0.063	0.000
RCM50	500	NaN	NaN	NaN	NaN	NaN	NaN	NaN	NaN
	5000	0.000	NaN	0.000	0.000	0.000	0.000	0.000	NaN
	50 000	0.000	NaN	0.000	0.303	0.090	0.000	0.000	0.000
	100 000	0.000	NaN	0.000	0.237	0.031	0.000	0.000	0.000

in order to reflect the impact of SUEA clearly. Experimental results are shown in Tables III-VI. When $HV_j(SUEA)$ is not zero whereas $HV_j(FPOP)$ is zero (i.e., the HV of the selected solution set from the UEA is not zero whereas the HV of the final population is zero), ∞ indicates that SUEA obtains feasible solutions while FPOP does not. When no feasible solutions are obtained (i.e., both FPOP and SUEA include no feasible solution), NaN is used. Due to the page limit, we only present part of the experimental results.

In Table III and Table IV, HVIR values in $(-1, 1)$ have no color, values in $[1, 10)$ are shaded in blue, values in $[10, 100)$ are shaded in yellow, and values in $[100, \infty)$ are shaded in red. Besides, NaN values are shaded in gray and ∞ values are shaded in green. That is, the colored cells show large improvements of HV values by subset selection.

C. Constrained EMO Algorithms

Based on the experimental results in Table III and Table IV, the following observations can be made:

- SUEA is effective in preserving feasible solutions, especially in early stage conditions.
- Negative effects of the SUEA are occasionally observed, they are infrequent.
- For CRE2-3-1 and RCM11, the HVIR values of C-MOEA/D increase as evaluation increases.

Regarding the first observation, the algorithms are in an early stage, resulting in the lack of feasible solutions in FPOP. The UEA can preserve the feasible solutions disregarded by FPOP, therefore the HVIR is non-negative for most problems.

Furthermore, due to the two-stage strategy and its stage-switching mechanism, PPS only transits from the push stage to the pull stage when the population shows no progress in convergence. Given the small number of generations, the algorithm remains in the push stage, where the population evolves without constraints. As a result, the whole FPOP of PPS may fall into infeasible regions for certain problems, whereas SUEA contains feasible non-dominated solutions, leading to ∞. This also proves the effectiveness of SUEA in preserving feasible solutions at early stages. In some circumstances, both SUEA and FPOP may lack feasible non-dominated solutions, resulting in NaN values. These phenomena are particularly common for problems containing a certain number of constraints.

The improvements of SUEA for C-MOEA/D on some real-world problems become more significant as the number of examined solutions increases. Since the preference for feasible solutions depends on the value of the PBI metric, this can be explained by [30], which suggested that the weight vectors used in decomposition-based algorithms are not suitable for the Pareto fronts of real-world problems. Thus, better solutions may be removed and SUEA provides significant improvements

TABLE V: HVIR for the three subset selection methods on the artificial problems.

Problem	Termination	CCMO	CTAEA	NSGAII	CMOEAD	PPS	CTSEA	CMME	CMOEA-MS
MW8	DSS	0.002	0.033	0.056	0.005	0.069	0.002	0.033	0.002
	LGI-HSS	0.015	0.046	0.070	0.018	0.122	0.014	0.046	0.015
	LGI-IGDSS	−0.030	−0.003	−0.005	−0.036	−0.030	−0.027	−0.004	−0.034
MW10	DSS	0.000	0.002	0.002	0.002	0.001	0.000	0.003	0.000
	LGI-HSS	0.001	0.003	0.002	0.003	0.003	0.001	0.004	0.001
	LGI-IGDSS	−0.018	−0.020	−0.013	−0.015	−0.011	−0.017	−0.018	−0.022
MW12	DSS	0.000	0.004	0.002	−0.001	0.003	−0.001	0.000	0.000
	LGI-HSS	0.001	0.007	0.004	0.000	0.005	0.001	0.002	0.002
	LGI-IGDSS	−0.007	−0.003	−0.005	−0.009	−0.005	−0.009	−0.007	−0.007
MW14	DSS	0.001	0.017	0.044	0.079	0.036	0.003	0.021	0.015
	LGI-HSS	0.024	0.038	0.067	0.101	0.056	0.023	0.043	0.039
	LGI-IGDSS	−0.054	−0.026	−0.017	−0.126	−0.127	−0.056	0.024	−0.086
LIR-CMOP1	DSS	0.000	0.000	0.000	0.115	0.003	0.000	0.001	0.000
	LGI-HSS	0.005	0.000	0.000	0.144	0.005	0.000	0.000	0.000
	LGI-IGDSS	−0.001	0.000	−0.004	0.102	−0.023	−0.001	0.000	−0.004
LIR-CMOP5	DSS	0.000	0.009	0.001	0.004	0.006	0.001	0.008	0.000
	LGI-HSS	0.002	0.008	0.003	0.006	0.006	0.003	0.010	0.002
	LGI-IGDSS	−0.008	−0.002	−0.016	−0.004	−0.001	−0.007	−0.004	−0.008
LIR-CMOP7	DSS	−0.001	0.007	0.004	0.006	0.005	0.000	0.008	−0.001
	LGI-HSS	0.003	0.008	0.007	0.007	0.007	0.003	0.009	0.003
	LGI-IGDSS	−0.009	0.004	−0.004	−0.004	−0.004	−0.010	−0.003	−0.010
LIR-CMOP9	DSS	0.000	0.011	0.000	0.062	0.001	0.000	0.002	0.098
	LGI-HSS	0.000	0.011	0.000	0.026	0.001	0.000	0.002	0.089
	LGI-IGDSS	−0.006	NaN	−0.005	0.051	−0.010	−0.005	−0.002	0.051
LIR-CMOP10	DSS	0.000	0.007	0.001	0.024	0.001	0.000	0.003	0.010
	LGI-HSS	0.000	0.007	0.001	0.017	0.001	0.001	0.004	0.009
	LGI-IGDSS	−0.010	−0.001	−0.022	0.002	−0.008	−0.009	−0.006	−0.004
LIR-CMOP14	DSS	0.006	0.018	0.264	−0.638	0.059	0.002	−0.153	0.003
	LGI-HSS	0.028	0.042	1.291	0.083	0.099	0.026	0.418	0.034
	LGI-IGDSS	−0.027	−0.008	0.863	0.021	0.022	−0.019	0.527	−0.030
C1-DTLZ1	DSS	−0.002	0.004	0.020	−0.001	0.020	−0.002	−0.001	0.001
	LGI-HSS	0.024	0.002	0.002	0.026	0.001	0.004	0.002	0.007
	LGI-IGDSS	−0.019	−0.012	−0.006	−0.024	−0.021	−0.018	−0.020	−0.019
C3-DTLZ4	DSS	−0.001	−0.002	0.029	−0.012	0.019	−0.001	0.000	0.481
	LGI-HSS	0.044	0.005	0.015	0.036	0.011	0.500	0.011	0.015
	LGI-IGDSS	−0.010	−0.011	0.014	−0.016	0.008	−0.008	−0.006	0.401

for C-MOEA/D.

Although the HV values of FPOP and SUEA are similar for most algorithms and problems, SUEA demonstrates its effectiveness in maintaining solution sets that outperform FPOP. As illustrated in Figure 1, while the HV value of SUEA is only slightly higher than that of FPOP for C-TAEA on LIR-CMOP9, SUEA exhibits better convergence and diversity compared to FPOP. This indicates that SUEA is effective in maintaining high-quality solution sets, even when the improvement in HV values (HVIR) is marginal.

The reasons why significant improvements are not common can be explained as follows. In early stages, the algorithms lack sufficient feasible non-dominated solutions to form effective UEAs for subset selection. In late stages, FPOPs of the algorithms have achieved good convergence and diversity. However, because the feasible regions are significantly smaller than the entire objective space, the solutions in FPOP and SUEA are concentrated in the same feasible regions. Consequently, these solutions are close in the objective space, limiting the effectiveness of HV-based subset selection for UEAs compared to its significant impact on unconstrained problems.

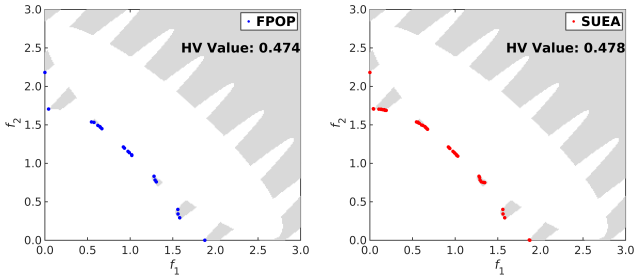

(a) (b)

Fig. 1: SUEA and feasible non-dominated solutions of FPOP of median HV run of C-TAEA on LIR-CMOP9 using LGI-HSS, number of solution evaluations is 50000. The gray areas are the feasible regions of LIR-CMOP9.

D. Different Subset Selections

Based on the experimental results in Table V and Table VI, the following observations can be made:

- Both DSS and LGI-HSS can achieve better performance than FPOP in most problems.
- Both DSS and LGI-IGDSS show degradation compared to LGI-HSS in most problems.
- LGI-IGDSS obtains the worst results and performs slightly worse than FPOP in some problems such as CRE3-6-2, MW8, and C1-DTLZ1.

From the experimental results, we notice that LGI-HSS achieves the best performance among the three subset selection methods in most problems. This is because we choose HVIR as the metric for evaluating the final performance. LGI-HSS aims to find a subset of solutions with the largest HV contribution, which guarantees that the selected subset can perform better on HV metric. Thus, the solutions obtained

TABLE VI: HVIR for the three subset selection methods on the real-world problems.

Problem	Selection Method	CCMO	CTAEA	NSGAII	CMOEAD	PPS	CTSEA	CMME	CMOEA-MS
CRE2-3-1	DSS	0.004	0.001	0.001	67.104	0.040	0.005	0.005	0.051
	LGI-HSS	0.005	0.000	0.001	65.534	0.040	0.005	0.005	0.053
	LGI-IGDSS	−0.005	0.000	−0.001	66.638	0.034	0.002	−0.005	0.041
CRE2-7-4	DSS	0.001	0.001	0.000	0.001	0.000	0.001	0.001	0.231
	LGI-HSS	0.001	0.001	0.001	0.001	0.001	0.001	0.001	0.128
	LGI-IGDSS	−0.002	0.000	0.000	−0.004	−0.001	−0.003	−0.006	0.228
CRE2-4-5	DSS	0.000	0.001	0.000	0.008	0.001	0.000	0.001	0.000
	LGI-HSS	0.000	0.001	0.000	0.008	0.000	0.000	0.001	0.000
	LGI-IGDSS	0.000	0.000	0.000	0.002	−0.004	0.000	0.000	−0.005
CRE3-7-1	DSS	0.029	0.037	0.061	5.547	0.087	0.033	0.038	0.030
	LGI-HSS	0.051	0.052	0.087	4.922	0.116	0.053	0.052	0.049
	LGI-IGDSS	0.015	0.006	0.039	0.988	−0.044	0.018	0.017	0.014
CRE3-6-2	DSS	0.000	0.012	0.007	0.113	0.007	0.001	0.018	0.627
	LGI-HSS	0.004	0.021	0.012	0.138	0.015	0.005	0.023	0.495
	LGI-IGDSS	−0.010	−0.021	−0.003	0.073	−0.002	−0.012	−0.036	0.578
RCM11	DSS	0.046	0.051	0.043	0.540	0.022	0.046	0.079	0.149
	LGI-HSS	0.068	0.064	0.063	0.570	0.038	0.064	0.093	0.166
	LGI-IGDSS	0.048	0.046	0.051	0.382	−0.004	0.049	0.064	0.142
RCM12	DSS	0.004	0.009	0.002	188.497	0.009	0.008	0.006	0.314
	LGI-HSS	0.004	0.009	0.002	1.364×10^3	0.008	0.006	0.005	0.360
	LGI-IGDSS	−0.008	0.000	−0.001	184.375	−0.004	−0.004	−0.004	0.289
RCM13	DSS	0.017	0.012	0.004	0.010	0.017	0.021	0.010	0.084
	LGI-HSS	0.025	0.012	0.013	0.011	0.020	0.027	0.013	0.118
	LGI-IGDSS	0.008	0.005	0.007	−0.059	0.012	0.014	0.004	0.079
RCM25	DSS	−0.001	0.000	0.003	0.027	0.001	−0.001	0.000	0.036
	LGI-HSS	−0.001	0.001	0.003	0.028	0.002	−0.001	0.001	0.036
	LGI-IGDSS	−0.013	−0.013	−0.009	0.000	−0.016	−0.012	−0.010	−0.003
RCM30	DSS	1.406	NaN	0.002	0.074	0.008	0.000	0.002	NaN
	LGI-HSS	0.000	NaN	0.000	0.043	0.013	0.000	0.001	NaN
	LGI-IGDSS	0.000	NaN	−0.007	0.056	0.006	−0.002	0.000	NaN
RCM50	DSS	0.000	NaN	0.000	0.303	0.015	0.000	0.000	0.000
	LGI-HSS	0.000	NaN	0.000	1.257	0.000	0.000	0.000	0.000
	LGI-IGDSS	0.001	NaN	0.000	0.865	−0.082	0.000	0.000	0.000

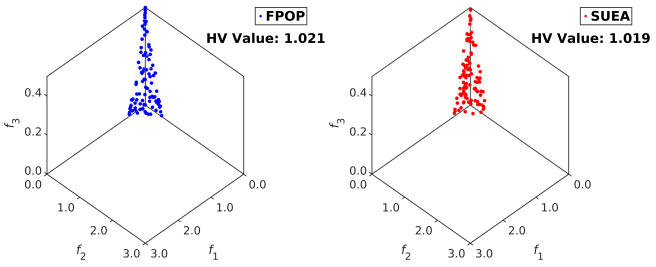

(a) (b)

Fig. 2: FPOP and SUEA of median HV run of PPS on C1-DTLZ1 using LGI-IGDSS, number of solution evaluations is 50000.

through LGI-HSS consistently show comparable stability or significantly better performance than the other two subset selection methods.

As for DSS, although it can achieve better performance than FPOP in most problems, its performance is still generally inferior to that of LGI-HSS. The degradation in the performance of DSS is more clearly observed in three-dimensional CMOPs such as MW14, LIR-CMOP14, and CRE3-7-1. This is because DSS focuses on selecting solutions to maximize the minimum Euclidean distance between solutions in the selected subset, which always leads to an evenly distributed subset in the objective space. However, since DSS performs selection based on solution spacing rather than the HV contribution, it tends to select distant solutions over those that may offer larger HV contributions. As a result, the subset might not capture the critical regions of the Pareto front that contribute most to the HV value, especially for high-dimensional CMOPs with more complex Pareto front geometries. In addition, unexpected performance may occur due to the "curse of dimensionality" [31]. In high-dimensional spaces, the relative differences between solution distances can be less pronounced, making it difficult for DSS to select the farthest solution for the solution subset. However, since most CMOPs are two-dimensional problems, selecting the farthest solutions can be effective to optimize the HV value in two-dimensional spaces, as they often define the extremes of the Pareto front.

For the limited performance of LGI-IGDSS, the algorithm tends to select a subset of solutions with the largest IGD+ contribution. IGD+ metric relies significantly on the specification of reference points to calculate the IGD+ value. However, in LGI-IGDSS, the reference points are set as the UEA itself. If some points in the reference set are unevenly distributed in the objective space or do not represent the critical regions of the Pareto front, these reference points may not be contributive in optimizing HV metric. As shown in Figure 2, SUEA selected by LGI-IGDSS exhibits less even distribution on the Pareto front compared to FPOP, leading to a marginally lower HV value. Since the UEA itself may contain suboptimal solutions, using these solutions as reference points can lead to derivation from the critical regions of the Pareto front, thereby performing worse than FPOP in some problems.

V. Conclusion

In this paper, we explored the effects of UEAs on the performance of eight constrained EMO algorithms. The ex-

perimental results demonstrated that UEAs are effective for constrained EMO algorithms in finding solution sets with better convergence and diversity compared to FPOP of each algorithm. The results also demonstrated that different subset selection methods also affect the performance of UEAs.

In the future, we intend to conduct further experiments to verify these conclusions and investigate any underlying reasons for the observed results, which may involve a deeper analysis of the UEA and various algorithmic components, as well as exploring alternative subset selection strategies that might better leverage the potential of the UEA.

ACKNOWLEDGMENT

This work was supported by National Natural Science Foundation of China (Grant No. 62376115, 62250710682), Guangdong Provincial Key Laboratory (Grant No. 2020B121201001).

REFERENCES

[1] K. Deb, *Multi-objective optimization using evolutionary algorithms*. USA: John Wiley & Sons, Inc., 2001.

[2] M. Li and X. Yao, "An empirical investigation of the optimality and monotonicity properties of multiobjective archiving methods," in *Evolutionary Multi-Criterion Optimization*, K. Deb, E. Goodman, C. A. Coello Coello, K. Klamroth, K. Miettinen, S. Mostaghim, and P. Reed, Eds. Cham: Springer International Publishing, 2019, pp. 15–26.

[3] T. Shu, K. Shang, H. Ishibuchi, and Y. Nan, "Effects of archive size on computation time and solution quality for multiobjective optimization," *IEEE Transactions on Evolutionary Computation*, vol. 27, no. 4, pp. 1145–1153, 2023.

[4] Y. Nan, T. Shu, and H. Ishibuchi, "Effects of external archives on the performance of multi-objective evolutionary algorithms on real-world problems," in *2023 IEEE Congress on Evolutionary Computation (CEC)*, 2023, pp. 1–8.

[5] K. Deb, S. Agrawal, A. Pratap, and T. Meyarivan, "A fast and elitist multiobjective genetic algorithm: NSGA-II," *IEEE Transactions on Evolutionary Computation*, vol. 6, pp. 182–197, 2002.

[6] H. Jain and K. Deb, "An evolutionary many-objective optimization algorithm using reference-point based nondominated sorting approach, part ii: Handling constraints and extending to an adaptive approach," *IEEE Transactions on Evolutionary Computation*, vol. 18, no. 4, pp. 602–622, 2014.

[7] F. Ming, W. Gong, L. Wang, and L. Gao, "A constrained many-objective optimization evolutionary algorithm with enhanced mating and environmental selections," *IEEE Transactions on Cybernetics*, vol. 53, no. 8, pp. 4934–4946, 2023.

[8] Z. Fan, W. Li, X. Cai, H. Li, C. Wei, Q. Zhang, K. Deb, and E. Goodman, "Push and pull search for solving constrained multi-objective optimization problems," *Swarm and Evolutionary Computation*, vol. 44, pp. 665–679, 2019.

[9] F. Ming, W. Gong, H. Zhen, S. Li, L. Wang, and Z. Liao, "A simple two-stage evolutionary algorithm for constrained multi-objective optimization," *Knowledge-Based Systems*, vol. 228, p. 107263, 2021.

[10] K. Li, R. Chen, G. Fu, and X. Yao, "Two-archive evolutionary algorithm for constrained multiobjective optimization," *IEEE Transactions on Evolutionary Computation*, vol. 23, no. 2, pp. 303–315, 2019.

[11] Y. Tian, T. Zhang, J. Xiao, X. Zhang, and Y. Jin, "A coevolutionary framework for constrained multiobjective optimization problems," *IEEE Transactions on Evolutionary Computation*, vol. 25, no. 1, pp. 102–116, 2021.

[12] H. K. Singh, K. S. Bhattacharjee, and T. Ray, "Distance-based subset selection for benchmarking in evolutionary multi/many-objective optimization," *IEEE Transactions on Evolutionary Computation*, vol. 23, no. 5, pp. 904–912, 2019.

[13] W. Chen, H. Ishibuchi, and K. Shang, "Fast greedy subset selection from large candidate solution sets in evolutionary multiobjective optimization," *IEEE Transactions on Evolutionary Computation*, vol. 26, no. 4, pp. 750–764, 2022.

[14] H. Ishibuchi, L. M. Pang, and K. Shang, "Solution subset selection for final decision making in evolutionary multi-objective optimization," *CoRR*, vol. abs/2006.08156, 2020.

[15] Y. Tian, Y. Zhang, Y. Su, X. Zhang, K. C. Tan, and Y. Jin, "Balancing objective optimization and constraint satisfaction in constrained evolutionary multiobjective optimization," *IEEE Transactions on Cybernetics*, vol. 52, no. 9, pp. 9559–9572, 2022.

[16] Y. Yuan, H. Xu, B. Wang, and X. Yao, "A new dominance relation-based evolutionary algorithm for many-objective optimization," *IEEE Transactions on Evolutionary Computation*, vol. 20, no. 1, pp. 16–37, 2016.

[17] T. Takahama and S. Sakai, "Constrained optimization by ϵ constrained particle swarm optimizer with ϵ-level control," in *Soft Computing as Transdisciplinary Science and Technology*, A. Abraham, Y. Dote, T. Furuhashi, M. Köppen, A. Ohuchi, and Y. Ohsawa, Eds. Berlin, Heidelberg: Springer Berlin Heidelberg, 2005, pp. 1019–1029.

[18] Z. Ma and Y. Wang, "Evolutionary constrained multiobjective optimization: Test suite construction and performance comparisons," *IEEE Transactions on Evolutionary Computation*, vol. 23, no. 6, pp. 972–986, 2019.

[19] Z. Fan, W. Li, X. Cai, H. Huang, Y. Fang, Y. Yugen, J. Mo, C. Wei, and E. Goodman, "An improved epsilon constraint-handling method in moea/d for cmops with large infeasible regions," *Soft Computing*, vol. 23, 12 2019.

[20] K. Deb, L. Thiele, M. Laumanns, and E. Zitzler, "Scalable multi-objective optimization test problems," *Proceedings of the 2002 Congress on Evolutionary Computation. CEC'02 (Cat. No.02TH8600)*, vol. 1, pp. 825–830 vol.1, 2002.

[21] S. Huband, P. Hingston, L. Barone, and L. While, "A review of multiobjective test problems and a scalable test problem toolkit," *IEEE Transactions on Evolutionary Computation*, vol. 10, no. 5, pp. 477–506, 2006.

[22] R. Tanabe and H. Ishibuchi, "An easy-to-use real-world multi-objective optimization problem suite," *Applied Soft Computing*, vol. 89, p. 106078, 2020.

[23] A. Kumar, G. Wu, M. Z. Ali, Q. Luo, R. Mallipeddi, P. N. Suganthan, and S. Das, "A benchmark-suite of real-world constrained multi-objective optimization problems and some baseline results," *Swarm and Evolutionary Computation*, vol. 67, p. 100961, 2021.

[24] Y. Nan, H. Ishibuchi, T. Shu, and K. Shang, "Analysis of real-world constrained multi-objective problems and performance comparison of multi-objective algorithms," in *Proceedings of the Genetic and Evolutionary Computation Conference*, ser. GECCO '24. New York, NY, USA: Association for Computing Machinery, 2024, p. 576–584.

[25] R. Tanabe, H. Ishibuchi, and A. Oyama, "Benchmarking multi- and many-objective evolutionary algorithms under two optimization scenarios," *IEEE Access*, vol. 5, pp. 19 597–19 619, 2017.

[26] E. Zitzler and L. Thiele, "Multiobjective optimization using evolutionary algorithms — a comparative case study," in *Parallel Problem Solving from Nature — PPSN V*, A. E. Eiben, T. Bäck, M. Schoenauer, and H.-P. Schwefel, Eds. Berlin, Heidelberg: Springer Berlin Heidelberg, 1998, pp. 292–301.

[27] H. Ishibuchi, H. Masuda, Y. Tanigaki, and Y. Nojima, "Modified distance calculation in generational distance and inverted generational distance," in *Evolutionary Multi-Criterion Optimization*, A. Gaspar-Cunha, C. Henggeler Antunes, and C. C. Coello, Eds. Cham: Springer International Publishing, 2015, pp. 110–125.

[28] Y. Tian, R. Cheng, X. Zhang, and Y. Jin, "PlatEMO: A MATLAB platform for evolutionary multi-objective optimization," *IEEE Computational Intelligence Magazine*, vol. 12, no. 4, pp. 73–87, 2017.

[29] H. Ishibuchi, R. Imada, Y. Setoguchi, and Y. Nojima, "How to specify a reference point in hypervolume calculation for fair performance comparison," *Evolutionary Computation*, vol. 26, no. 3, pp. 411–440, 09 2018.

[30] H. Ishibuchi, Y. Setoguchi, H. Masuda, and Y. Nojima, "Performance of decomposition-based many-objective algorithms strongly depends on pareto front shapes," *IEEE Transactions on Evolutionary Computation*, vol. 21, no. 2, pp. 169–190, 2017.

[31] D. Peng, Z. Gui, and H. Wu, "Interpreting the curse of dimensionality from distance concentration and manifold effect," *CoRR*, vol. abs/2401.00422, 2024.